Kinetics Processivity and the Direction of Motion of Ncd

E. Pechatnikova and E. W. Taylor
Department of Molecular Genetics and Cell Biology, The University of Chicago, Chicago, Illinois 60637

ABSTRACT The kinetic mechanism of the nonclaret disjunctional protein (Ncd) motor was investigated using the dimer termed MC1 (residues 209–700), which has been shown to exhibit negative-end directed motility (Chandra et al., 1993). The kinetic properties are similar to those of the monomeric Ncd motor domain (Pechatnikova and Taylor, 1997). The maximum steady-state ATPase activity of 1.5 s^{-1} is half as large as for the monomeric motor. Dissociation constants in the presence of nucleotides showed the same trend but with approximately a two-fold decrease in the values: K_d values are 1.0 μM for ADP-AlF_4, 1.1 μM for ATPγS, 1.5 μM for ATP, 3 μM for ADP, and 10 μM for ADP-vanadate (in 25 mM NaCl, 22°C). The apparent second-order rate constants for the binding of ATP and ADP to the microtubule-motor complex (MtMC1) are 2 μM^{-1} s^{-1}. Based on measurements at high microtubule concentrations the kinetic steps were fitted to the scheme,

$$\mathrm{MtN} + \mathrm{T} \underset{}{\overset{k_1=110s^{-1}}{\rightleftharpoons}} \mathrm{MtN{\cdot}T} \overset{k_2=20s^{-1}}{\rightleftharpoons} \mathrm{MtN{\cdot}D{\cdot}P} \overset{k_3=10s^{-1}(-\mathrm{P})}{\rightleftharpoons} \mathrm{MtN{\cdot}D} \underset{k_{-4}=200s^{-1}}{\overset{k_4=6s^{-1}}{\rightleftharpoons}} \mathrm{MtN} + \mathrm{D},$$

where N refers to one head of the dimer and T, D, and P stand for ATP, ADP, and inorganic phosphate. k_1 and k_{-4} are the first-order rate constants of the transition induced by the binding of mant ATP and mant ADP respectively. ADP release is the main rate-limiting step in the MtMC1 mechanism. The binding of the MC1–mant ADP complex to microtubules released less than half of the mant ADP (alternating site reactivity). The second mant ADP is only released by the binding of nucleotides that dissociate the MtMC1 complex (ATP and ADP but not AMPPNP). The apparent rate constant for dissociation of the second mant ADP is four times smaller than the first and much smaller than the rate of dissociation of MtMC1 by ATP or ADP. These results are explained by a model in which MC1·ADP is first dissociated from the microtubule by ATP, followed by rebinding to the microtubule by the ADP-containing head. Ncd may follow a different reaction pathway than does kinesin, but the differences in rate constants do not explain the opposite direction of motion. The kinetic evidence and the high ratio of motile velocity to ATPase support a nonprocessive, low duty cycle mechanism for the Ncd motor.

INTRODUCTION

The nonclaret disjunctional protein (Ncd) is a member of the group of microtubule-associated motors that have the motor domain at the C terminal end of the protein and move in the negative direction along the microtubule. The structures of the motor domains of conventional kinesin and Ncd are very similar (Sablin et al., 1996; Kull et al., 1996), yet the motors move in opposite directions along a microtubule. The velocity of microtubule movement produced by full-length Ncd or dimeric constructs is more than five times slower than kinesin, and the ATPase activity is more than ten times smaller (Chandra et al., 1993). A further difference in properties is that the kinesin dimer shows a high degree of processivity, whereas processivity has not been demonstrated for Ncd by either the dilution assay or the single molecule assay (Chandra et al., 1993; Vale et al., 1996; Case et al., 1997). We define the degree of mechanical processivity as the number of movement steps per encounter of the motor with the microtubule, and the degree of kinetic processivity as the number of ATPase cycles per head per encounter.

These findings raise a number of questions. Which properties of the proteins determine whether the behavior is processive? Because processivity is a competition between detachment of one head to take a movement step and dissociation of both heads, the answer should be given by determining the kinetic mechanism. Studies on the ATPase mechanism showed that Ncd and kinesin share some essential features. In the absence of microtubules, the rate-limiting step is ADP dissociation (Shimizu et al., 1995b). The rate of the hydrolysis step is much larger than the steady-state turnover rate, which gives rise to a phosphate burst (Pechatnikova and Taylor, 1997). The binding Ncd to the microtubule accelerates the rate of ADP release. A comparison of the rate of dissociation of ADP with the maximum ATPase rate for conventional kinesin, Ncd and Eg5, showed the ratio to be a factor of 1.5 to 2 (Ma and Taylor, 1995; Shimizu et al., 1995b; Lockhart et al., 1995; Lockhart and Cross, 1996; Ma and Taylor, 1997a; Pechatnikova and Taylor, 1997). It was proposed that this correlation is characteristic of kinesin family motors. However, Gilbert et al. (1995) obtained a much larger ratio and they concluded that

Received for publication 3 August 1998 and in final form 18 May 1999.

Address correspondence and reprint requests to E. W. Taylor, Department of Molecular Genetics and Cell Biology, University of Chicago, 920 E. 58th St., Chicago, IL, 60637. Tel.: 773-702-1660; Fax: 773-702-3172; E-mail; ewt1@midway.uchicago.edu.

Abbreviation used: Ncd, Ncd constructs of R335–K700 amino acid residues; AMPPNP, 5′-adenylyl β,γ-imidodiphosphate; mant ATP and mant ADP, 2′-(3′)-O-(*N*-methylanthraniloyl) adenosine 5′-triphosphate and 5′-diphosphate, ATPγS, adenosine 5′-O-(3-thiotriphosphate); PIPES, 1,4-piperazinediethanesulfonic acid; Mt, microtubule.

0006-3495/99/08/1003/14 $2.00

ADP dissociation does not contribute to the rate-limiting steps.

Despite these similarities, there are significant differences in the kinetic mechanisms of kinesin and Ncd. A monomeric Ncd construct (amino acids 335–700) was previously investigated and compared to a monomer of conventional kinesin (Pechatnikova and Taylor, 1997). The rate constants for the hydrolysis and ADP release steps are ten to twenty times smaller for Ncd than for kinesin, but the rate of dissociation of the MtNcd monomer by ATP or ADP is similar to kinesin. In the ATPase cycle, the rate of dissociation of the MtNcd·ADP complex into Mt plus Ncd·ADP is larger than the rate of dissociation into MtNcd plus ADP. In the case of kinesin, the rate of ADP dissociation is larger than the rate of dissociation of the kinesin·ADP complex from the microtubule; consequently, monomeric kinesin exhibits kinetic processivity (Ma and Taylor, 1997a; Jiang and Hackney, 1997; Moyer et al., 1998). Although this comparison was made between monomers that are not mechanically processive, these differences in the reaction pathway are expected to be significant in determining whether or not a dimeric motor is processive.

The present work was undertaken to determine the kinetic properties of a dimeric Ncd. Conventional kinesin showed striking differences in kinetics between monomer and dimer for the ATP and ADP binding and release steps (Ma and Taylor, 1997a,b). These differences are explained by the negative interaction between heads on the microtubule lattice discovered by Hackney (1994). The binding of a dimeric kinesin–ADP complex to a microtubule releases ADP from only one head. The ADP is released from the second head by the binding of ATP, or other nucleotides, to the first head. This interaction tends to keep the ATPase cycles partly out of phase on the two heads, and thus favors processivity by having one or the other head strongly bound throughout most of the cycle (Hackney, 1994; Ma and Taylor, 1997b; Gilbert et al., 1998). An important question is whether the Ncd dimer shows the same negative interaction.

Dimeric Ncd constructs were first prepared by Chandra et al. (1993). These constructs, termed MC1 and MC5, were shown to produce microtubule gliding at rates comparable to full-length Ncd. The studies reported here show that MC1, like kinesin, releases only one ADP on binding to microtubules, and the second ADP is released by reaction with ATP. A comparison of the kinetic data on the monomer and the dimer supports the conclusion that there is a negative interaction between heads of the dimer. However, MC1 and kinesin probably follow different reaction pathways for the release of the second ADP.

Image reconstructions of microtubule–Ncd complexes indicate that only one head is bound to the microtubule (Hirose et al., 1996; Sosa et al., 1997). Although the two heads are identical before interaction with the microtubule, the bound head is expected to have altered affinity for nucleotides. Kinetic studies are in agreement with the structural evidence. The kinetic behavior is consistent with a mechanism in which only one head is bound to the microtubule, and the attached and detached heads have different affinity for ATP and ADP.

An intriguing problem is the opposite direction of motion of kinesin and Ncd. Recent studies have shown differences in structure in the neck region (Kozielski et al., 1997; Sablin et al., 1998). The Ncd head, connected to the kinesin neck, moves slowly in the positive direction (Henningsen and Schliva, 1997; Case et al., 1997, 1999), whereas the kinesin head joined to the Ncd neck moves very slowly in the negative direction (Endow and Waligora, 1998). Kinesin and Ncd also show significant differences in the relative values of rate constants for some steps in the reaction, which could alter the pathway. The kinetic evidence allows a discussion of the question whether differences in the reaction pathway contribute to determining the direction of motion.

MATERIALS AND METHODS

Expression and purification of proteins

The MC1 motor domain, R209–K700 plus a Gst domain at the N terminal, was prepared from BL21 (DE3) host cells transformed by the recombinant plasmid pGEX-MC1, provided by Y. Y. Toyoshima. Protein was purified as described previously for the Ncd monomer (Shimizu et al., 1995b); the clarified cell lysate was chromatographed on S-Sepharose FF using a gradient of 50 mM to 400 mM NaCl in 10 mM sodium phosphate buffer, pH 7.4, 2 mM $MgCl_2$, 1 mM EGTA, 4°C. The fractions containing MC1 were pooled, ATP was added at a 1:1 molar ratio, and the protein was precipitated with 50% ammonium sulfate. The protein pellet was resuspended in a small volume of standard buffer (25 mM PIPES, pH 6.9, 2 mM $MgCl_2$, 1 mM EGTA) and 75 mM NaCl, and 2 mM ATP were added. The solution was dialyzed overnight at 4°C against the standard buffer plus 75 mM NaCl. Ten percent sucrose and one mole ATP per mole MC1 were added, and the protein was stored at −80°C. The purity, based on SDSPAGE, was generally higher than 85%. In some experiments, a microtubule–MC1 complex was pelleted and resuspended to remove unbound MC1. The relative molecular weight per site is 83,400 based on the sequence (Chandra et al., 1993).

The purification of tubulin from porcine brain and the preparation of microtubules were described in Ma and Taylor (1995). Microtubules were sedimented through a 30% glycerol cushion at 37°C to remove free GTP and GDP, resuspended, and subjected to a low-speed spin to remove large aggregates. Taxol at a concentration of 15 μM was present in all solutions of microtubules. ^{3}H-MC1 was obtained by reaction with *N*-succinimidyl[2,3-^{3}H]propionate (Amersham,) as described in Ma and Taylor (1995).

A nucleotide-free MC1–microtubule complex was obtained by treatment with apyrase (Grade VII, Sigma,) in standard buffer plus 50 mM NaCl. An apyrase concentration of 0.003 mg/mL was sufficient to release all bound ADP in 40 min at room temperature from 40 μM MC1–microtubule complex as assayed by the decrease in fluorescence of bound mant ADP. The solution was diluted with buffer or buffer plus microtubules just before use. Hydrolysis of ATP or ADP by this concentration of apyrase can be neglected in most of the transient kinetic experiments. In some cases the MC1–microtubule complex was sedimented and resuspended to remove apyrase and free phosphate.

The mutant phosphate-binding protein (A197C) was prepared from *Escherichia coli* strain ANCC75 containing the plasmid pSN5182/7. The strain was provided through the courtesy of M. R. Webb, MRC, Mill Hill, London. The protein was purified and labeled with MDCC, (*N*-[2-(1-maleimidyl)-7-(diethylamino)coumarin-3-carboxamide]) (obtained from Molecular Probes,) by the method of Brune et al. (1994).

Binding of MC1 to microtubules

The binding was measured by a sedimentation method using ^{3}H-MC1 (Ma and Taylor, 1995). The labeled MC1 was centrifuged for 15 min at maximum speed in a Beckman airfuge to remove any aggregates. Nucleotide and microtubules were added to the MC1 and the solution was centrifuged for 15 min at 22°C. For each series of experiments at different microtubule concentrations, one centrifugation was carried out in 1 mM AMPPNP. The binding runs in different experiments were normalized to the binding in the presence of AMPPNP.

Transient kinetic experiments

Nucleotide binding and dissociation were measured using fluorescent substrate analogs, 2′(3′)-O-(*N*-methylanthraniloyl) ATP and ADP, which were prepared by the method of Ma and Taylor (1995). The purity of the various samples was checked by thin layer chromatography on silica plates in 1-propanol/NH_4OH/H_2O, 6:3:1 by volume plus 0.5 g/L EDTA.

An MC1·mant ADP complex was prepared by overnight dialysis of MC1 against mant ATP at 4°C at a ratio of total nucleotide to protein sites of 20. A 90 to 95% exchange of mant ADP for ADP was obtained. Free mant ADP was removed by sedimentation over a G-25 spin column at 4°C just before the experiments. The MC1 had at least 0.8 moles of mant ADP bound per mole of MC1 sites, determined by measurement of the fluorescence intensity after displacement of mant ADP by excess ATP. The fluorescence enhancement ratio is defined as the fluorescence intensity per mole bound mant ADP divided by the fluorescence intensity per mole free mant ADP. The value is 1.8 ± 0.1 measured in the fluorimeter at 22°C.

Stop-flow and chemical quench-flow measurements were made as described previously (Ma and Taylor, 1995). Slow reactions of mant ADP or mant ATP were measured in a Perkin-Elmer MPF 44A fluorimeter (excitation, 365 nm; emission, 440 nm). In stop-flow experiments, the same wavelengths were obtained using interference filters. ATPase activity was determined using [γ-^{32}P]ATP. The reaction was stopped by mixing with HCl at a final concentration 0.7 N. The [^{32}P] P_i produced by hydrolysis was separated from unreacted nucleotide on charcoal columns. The fractional hydrolysis was calculated from the ratio of sample counts to total counts as described previously (Ma and Taylor, 1995). At least three time points were taken for steady-state rate measurements.

The kinetic mechanism was simulated using the KINSIM program.

RESULTS

Steady-state properties of MC1

MC1 has a very small ATPase activity of 0.001 s^{-1} per site. The rate constant of ADP dissociation was determined using the fluorescence enhancement of bound mant ADP, which decreased when mixed with ATP, with a rate constant of 0.0014 s^{-1}. The same rate constant was obtained using apyrase to degrade free mant ADP. The results confirm previous studies with monomeric Ncd showing that ADP release is the rate-limiting step. The turnover rate is 3 times larger than for monomeric Ncd (Pechatnikova and Taylor, 1997).

In the presence of microtubules, the maximum rate per site (V_M), obtained by fitting the dependence on microtubule concentration to a hyperbola, is 1.5 s^{-1} in 25 mM NaCl and 20°C. The tubulin dimer concentration at half maximum rate, K_M(Mt), is 6 μM. The maximum rate decreased to 0.7 s^{-1} in 50 mM NaCl and the K_M(Mt) increased markedly when the ionic strength was increased. The values are in the range reported for MC-5 (Lockhart et al. 1995). The steady-state ATPase of MtMC1, as a function of ATP concentration, measured at 30 μM Mt in 50 mM NaCl gave a K_M(ATP) of 35 μM, which is the same as for monomeric Ncd. The steady-state properties are summarized in Table 1.

The affinity of MC1 for microtubules was measured with the microtubule site concentration in large excess to avoid effects of lattice occupancy. In the absence of free ADP or in the presence of 1 mM AMPPNP, the maximum binding of the MC1 was higher than 80% for the preparations used in the experiments. The unbound fraction consists of some impurities and inactive protein. For most experiments, the MtMC1 complex was sedimented and resuspended to remove impurities. The maximum binding of the recycled material approached 100% in the presence of AMPPNP.

The binding of various MC1-nucleotide complexes to microtubules was measured in standard buffer pH 6.9, 25 mM NaCl, 22°C. Binding curves (Fig. 1) in the presence of 0.5 mM ATPγS or ADP-AlF_4 (2 mM ADP plus 2 mM AlF_4) extrapolated to a maximum of 0.95 to 1.0 with dissociation constants (K_d) of 1.1 μM and 0.8 μM, respectively. However, in the presence of 5 mM ATP or 5 mM ADP, the binding extrapolated to 0.6, and the value was even lower for ADP-vanadate (2 mM ADP plus 1 mM vanadate). The high ATP concentration was used to ensure that the substrate was not depleted during sedimentation of the complex, and binding was measured at the same ADP concentration for comparison. The use of higher concentrations of $MgCl_2$ and nucleotide increases the ionic strength, but measurements at 2 mM ADP were not significantly different. A smaller value for the maximum binding of weakly bound complexes was also observed for monomeric Ncd (Pechatnikova and Taylor, 1997). MC1 was sedimented with microtubules in the presence of ADP and used for a second binding experiment. The maximum binding was essentially unchanged, which indicates that the explanation is not that the MC1 is heterogeneous.

TABLE 1 Steady-state rate constants and dissociation constants of Mt-MCl*

V_M (s^{-1})	K_M(Mt)	K_M(ATP)	K_d [ATP]	K_d [ADP]	K_d [ATPγS]	K_d [ADP-AlF_4]	K_d [ADP-Vanadate]
1.5	6 μM	40 μM	1.5 μM	3 μM	1.1 μM	1.0 μM	10 μM

*Dissociation constants are expressed as tubulin dimer concentration. K_M(Mt), tubulin dimer concentration for half-maximum ATPase activation; V_M, extrapolated maximum ATPase rate per MCl site; K_d, dissociation constant of Mt-MCl in the presence of a nucleotide or nucleotide analog. Data given are averages of three or four measurements per point fitted to a hyperbola. Conditions: 25 mM PIPES, pH 6.9, 1 mM EGTA, 2 mM $MgCl_2$, 25 mM NaCl, 22°C. ATPase was measured in 0.5 mM MgATP (0.5 mM ATP plus 0.5 mM $MgCl_2$). The binding in the presence of ATP or ADP was measured in 5 mM MgATP or 5 mM MgADP; the binding in the presence of analogs was measured in 0.5 mM ATPγS, in 2 mM MgADP plus 1 mM sodium vanadate or in 2 mM MgADP plus 2 mM AlF_4 (2 mM $AlCl_3$, 10 mM NaF, NaCl concentration reduced to 15 mM).

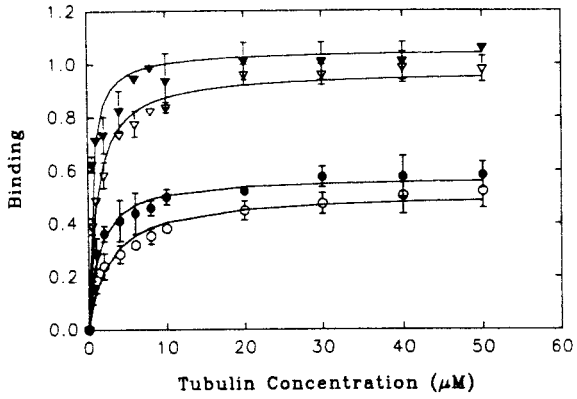

FIGURE 1 Binding of MC1 to microtubules in the presence of nucleotides. The binding of [^{3}H] MC1 was measured by a sedimentation assay. Each curve is the unconstrained fit of binding data to a hyperbola. Error bars refer to standard deviations of three or four measurements. (▼), 2 mM MgADP plus 2 mM AlF_4; (▽), 0.5 mM ATPγ S; (●), 5mM MgATP; (○), 5 mM MgADP. Conditions: 25 mM PIPES, pH 6.9, 25 mM NaCl, 1 mM EGTA, 2 mM $MgCl_2$; 1 μM MC1, 22°C. Dissociation constants are given in Table 1.

The dissociation constants obtained from an unconstrained fit (Table 1) may reduce the actual difference between strongly and weakly bound complexes. However, the general trend in dissociation constants is clear: the same ordering of the magnitudes of the dissociation constants was obtained previously for monomeric Ncd and conventional kinesin (Ma and Taylor, 1995). The results are also in general agreement with those of Crevel et al. (1996).

The MC1·ATPγS complex, which may be an analog of an ATP complex, is strongly bound. The MC1·ADP complex is relatively weakly bound, and the affinity is further reduced by the presence of vanadate. However, the results for the ADP–AlF_4 and ADP–vanadate complexes are difficult to interpret.

Both complexes could be analogs of an ADP–phosphate complex. Because phosphate dissociates MtMC1·ADP, the binding of MC1·ADP·phosphate to microtubules is expected to be weaker than MC1·ADP (Foster et al., 1998). However, kinesins may be more closely related to G proteins than to myosin in terms of the interaction of their nucleotide complexes with microtubules. The nucleoside triphosphate state is strongly bound while the diphosphate state is weakly bound to the microtubule. The MC1·ADP·AlF_4 complex may be an analog of the triphosphate state, just as the GDP·AlF_4 complex is a triphosphate analog in the case of G proteins. The weak binding of MC1 to microtubules in the presence of ADP plus vanadate requires further investigation because there is no evidence that vanadate binds at the active site to form a stable complex. The addition of 1 mM vanadate to MC1·mant ADP did not affect the rate of release of the mant ADP by the addition of microtubules plus ATP. The corresponding experiment with MC1·mant ADP·AlF_4 gave a 2.5-fold smaller rate of mant ADP dissociation, which is a change in the expected direction.

The dissociation constants increased markedly with increasing ionic strength. The values in 50 mM NaCl are approximately two times larger than in 25 mM NaCl.

Kinetic studies of the microtubule-MC1 ATPase mechanism

Kinetic studies require the strongly bound ADP to be removed from MC1, but treatment with EDTA or apyrase led to precipitation and denaturation. The protein is marginally stable in a nucleotide-free form when bound to microtubules, as was noted previously for monomeric Ncd. As described in the section on ADP dissociation, less than half of the bound ADP was released from MC1 on forming a complex with microtubules. The presence of some bound ADP complicated the transient kinetic behavior because the ADP is slowly released in competition with the binding of fluorescent or radioactive nucleotides. In most experiments, the bound ADP was removed by treatment with apyrase, but this treatment does lead to some loss in nucleotide binding sites. Sedimentation and resuspension of the nucleotide-free complex led to the loss of some MC1 that may have been denatured during the treatment.

The fluorescence enhancement ratio per nucleotide binding site is 1.8 measured in the fluorimeter and 1.6 to 1.7 in the stop-flow apparatus. Before apyrase treatment of the MtMC1 complex, the MC1 typically binds 0.8 to 0.9 M nucleotide per mole of MC1 sites. The expected fluorescence enhancement ratio is 1.5, but the maximum enhancement ratio obtained in transient kinetics experiments is 1.4, expressed relative to the original MC1 site concentration, which indicates some loss of binding sites by treatment with apyrase.

Binding of mant ATP to MtMC1

The fluorescence enhancement for the binding of mant ATP is illustrated in Fig. 2 *a* for a mant ATP concentration of 40 μM (15 μM microtubules, 15 μM MC1, standard buffer plus 50 mM NaCl, 22°C). The signal fitted one exponential term with a rate constant of 59 s^{-1}.

The increase in fluorescence relative to the value at zero time is plotted on an arbitrary scale that is proportional to photomultiplier output voltage. The enhancement ratio is obtained from $(\Delta V/V_{initial})$[mant ATP]/[MC1] where V is photomultiplier output voltage and [mant ATP]/[MC1] is the concentration ratio.

Measurements over a wide range of concentrations gave complex results. At low substrate concentrations, the fluorescence signal fitted two exponential terms. The smaller rate process contributed approximately 50% of the signal at 2 μM mant ATP, but the contribution decreased with concentration and this step was not detected for concentrations greater than 30 to 40 μM. Both rate constants are plotted in Fig. 2 *b*. The smaller rate constant increased with concentration to about 10 s^{-1}, but the maximum rate is probably

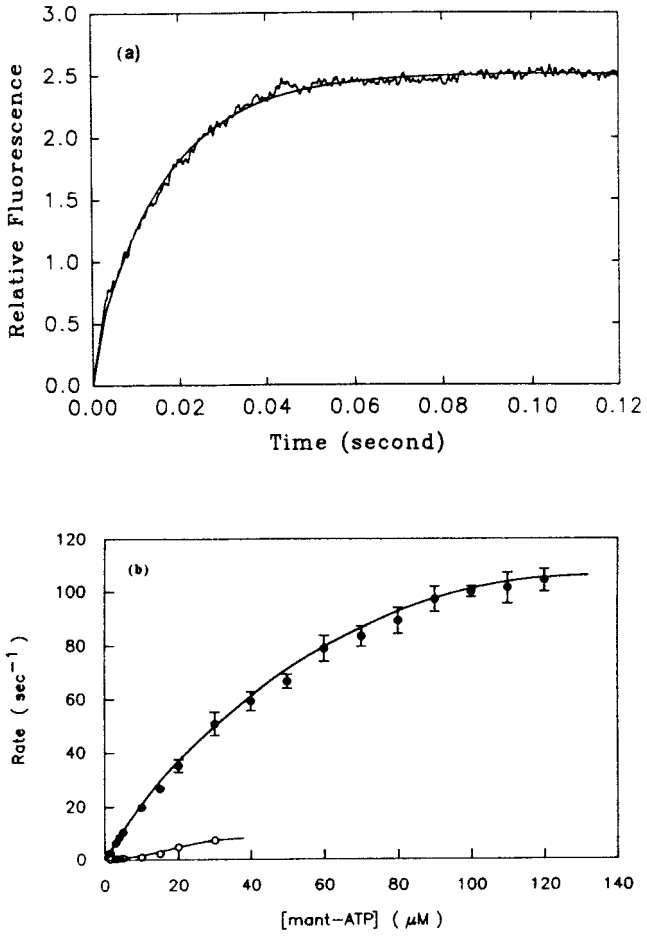

FIGURE 2 (*a*) Time course of the fluorescence enhancement for the reaction of mant ATP with the MtMC1 complex. The jagged curve is the fluorescence signal for the binding of mant ATP at a concentration of 40 μM. The smooth curve is the fit to one exponential term; the rate constant is 59 s^{-1}. Conditions: standard buffer, 50 mM NaCl, 22°C, 15 μM MC1, 15 μM microtubules (tubulin dimer concentration). In all stop-flow experiments, protein and nucleotide concentrations are final concentrations after mixing 1:1 in the apparatus. The microtubule-MC1 complex was treated with 1 unit per mL of apyrase for 40 min just before the experiment. Fluorescence is plotted on an arbitrary scale; the increase in fluorescence emission is 15% relative to the value at zero time. (*b*) Concentration dependence of the apparent rate constants for the binding of mant ATP to the MtMC1 complex. The apparent rate constants were obtained by fitting the data to two exponential terms at low mant ATP concentration and to one exponential at concentrations greater than 30 μM. The process with the larger rate constant (●) fitted a hyperbolic dependence on mant ATP concentration that extrapolated to a maximum rate of 110 s^{-1}; the initial slope is 2 μM^{-1} s^{-1}. The smaller rate process (○) probably increased to at least 10 s^{-1} but the signal became too small to fit before the maximum was reached. Error bars refer to the range of three to five measurements. Conditions: standard buffer, 50 mM NaCl, 22°C.

larger. The process with the larger rate constant increased to a maximum of 100 to 120 s^{-1} with an initial slope of 2 μM^{-1} s^{-1}. The concentration for half maximum rate is 35 to 40 μM, which is the same as the value for K_M(ATP).

The total fluorescence enhancement also increased with concentration in the range from 2 to 10 μM, which indicates a site with an effective dissociation constant of about 5 μM.

A plausible explanation of the kinetic behavior can be given in terms of two classes of nucleotide binding sites corresponding to detached and attached heads. The detached head, with high affinity for mant ATP, dominates the fluorescence signal at very low substrate concentrations and contributes only to the larger rate constant. The attached head, with lower affinity for mant ATP, is expected to give a biphasic fluorescence signal and to contribute to both rate processes. A detailed treatment of the mechanism is given in the Conclusions section.

The binding of mant ADP to MtMC1 gave results that were essentially the same as for the MtNcd monomer complex. The signal was biphasic at low concentrations, but fitted a single rate constant at high concentrations. The rate constant of the main signal showed a hyperbolic dependence on concentration with an initial slope of 1.8 μM^{-1} s^{-1} and a maximum rate of 200 s^{-1}.

Hydrolysis and phosphate dissociation steps

The MtMC1 complex that had been pretreated with apyrase exhibited a phosphate burst phase (Fig. 3). Under the experimental conditions of a microtubule concentration of 30 μM in 50 mM NaCl, the complex should remain largely associated during the transient phase. The data were fitted to one exponential plus a linear term. Measurements were continued for several seconds using the quench-flow apparatus to determine the linear (steady-state) rate. The steady-state rate was also measured by mixing by hand. The hydrolysis of ATP by apyrase, measured under the same conditions, contributed approximately 20% to the steady-state rate. In 75 μM ATP, the rate constant of the transient phase was 20 $\pm$ 3 s^{-1} and the amplitude was 0.4 $\pm$ 0.03

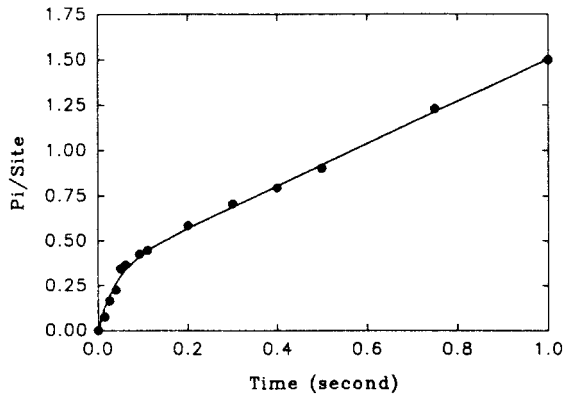

FIGURE 3 Phosphate burst phase of MtMC1 complex. The early time course of ATP hydrolysis by MtMC1 was measured in a quench-flow apparatus. Phosphate formation is expressed per MC1 site. Data are plotted for the first second, but measurements were continued for several seconds. The MtMC1 complex was treated with 1 unit per mL apyrase for 40 min just before starting the experiment. The data points are averages of three or four measurements. The steady-state rate is 1.2 s^{-1}; the transient rate constant is 23 s^{-1}; the burst size is 0.4 (psi plot program, data fitted to one exponential plus a linear term). Conditions: standard buffer, 50 mM NaCl, 10 μM MC1, 30 μM Mt, 75 μM [γ-^{32}P] ATP, 25°C.

(average of four experiments). The corrected steady-state rate was 1 s^{-1}.

The rate constant of the burst phase was slightly larger than the value of 15 s^{-1} obtained for the monomer, but the values agree within experimental error. The burst phase was measured at 100, 150, and 250 μM ATP concentrations. The rate constants were not significantly larger than in 75 μM ATP, although the error was larger at higher concentrations because the fractional hydrolysis during the transient phase was smaller. The maximum rate for saturating ATP was 23 s^{-1}. In 150 mM NaCl, a burst phase was still obtained with a rate constant of 20 s^{-1}. At this ionic strength, the MtMC1 complex was almost completely dissociated at the end of the transient phase.

The size of the phosphate burst was measured for a range of ionic strengths and ATP concentrations. In the quench-flow apparatus the burst was less than one per site. In some experiments the transient phase was better fitted by two exponential terms, but in general the errors were too large to justify fitting an additional rate constant. The burst size, obtained by extrapolation of the steady-state rate, measured by mixing by hand, gave a value of 1.1 $\pm$ 0.2 (5 measurements) at high ionic strength (150 mM NaCl). In 25 mM NaCl, the burst amplitude was 1.5 $\pm$ 0.3.

Because the values were not corrected for loss of active sites by apyrase treatment, the size of the burst may be underestimated. If the complex was not treated with apyrase, the size of the burst measured in the quench-flow apparatus was less than 0.5, but extrapolation from the steady state gave 0.8 (in 150 mM NaCl). On the basis of the results for mant ADP dissociation described below, less than half of the ADP would be released by binding to microtubules at the concentration of MC1 used in these experiments. The dissociation of the remainder of the ADP at a rate that is larger than the steady-state turnover rate would increase the size of the burst, as measured by extrapolation from the steady state.

The rate of phosphate dissociation was measured using the phosphate-binding protein of Brune et al. (1994). A burst of phosphate release was obtained at low ionic strength and high microtubule concentration, conditions that favor association of the MtMC1 complex (Fig. 4). At an ATP concentration of 100 μM, the rate constant of the burst obtained by fitting to one exponential plus a linear term was 8 $\pm$ 1 s^{-1}, and the amplitude was 0.15 $\pm$ 0.03 M per mole of sites. The results are average values for two preparations of MC1.

The MtMC1 complex was not treated with apyrase and the fraction of ADP-free sites is expected to be 0.3 to 0.4. There was a lag phase, but it was too small to obtain a reliable fit to two exponential terms. A lag is expected because the rate of the hydrolysis step is only 20 s^{-1}. Sedimentation and resuspension of the MtMC1 complex to remove free ADP and any MC1 that did not bind to microtubules increased the burst size but did not affect the rate constant.

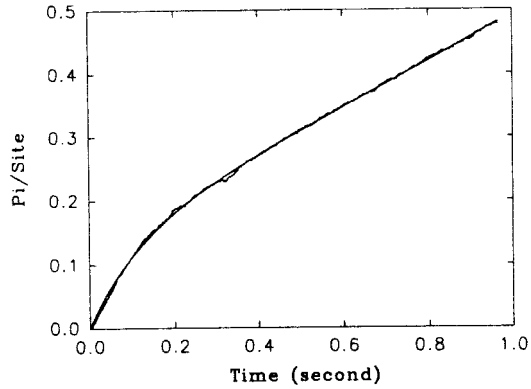

FIGURE 4 Dissociation of phosphate during the transient phase. The MtMC1 complex was reacted with ATP in the presence of the fluorescent phosphate binding protein. Conditions: standard buffer, 25 mM NaCl, 4 μM MC1, 25 μM microtubules, 100 μM ATP, concentrations after mixing. Both syringes contained 10 μM phosphate binding protein, 200 mM methylguanosine, 0.1 units per mL nucleoside phosphorylase. The MtMC1 complex was not pretreated to remove bound ADP. Rate constant of the initial phase is 8.7 s^{-1}; burst amplitude 0.12; steady-state rate 0.36 s^{-1}. The amplitude of the fluorescence change was converted to phosphate concentration by comparison with the fluorescence change for the reaction of the phosphate binding protein with inorganic phosphate in the stop-flow apparatus.

Measurements were also made on monomeric Ncd under the same conditions of low ionic strength and high microtubule concentration. At 100 μM ATP, the rate of the burst phase was 8 to 10 s^{-1} with an amplitude of 0.15 to 0.2 per site. These results support the conclusion that the burst is obtained from the head, which is strongly bound to the microtubule.

Despite the high microtubule concentration, there is some dissociation of MC1 by ATP with a rate constant of at least 10 s^{-1} that complicates the interpretation of the burst phase. A part of the phosphate could be released after dissociation of MC1·ADP·P. At 150 mM NaCl and 2 μM microtubules, the system dissociates during the transient phase. A phosphate release burst was observed with rate of 5 s^{-1} but the amplitude was reduced by a factor of two. Therefore, partial dissociation may lead to an underestimation of the rate constant of phosphate dissociation from MtMC1·ADP·P. The results for MC1 are in contrast to processive kinesin, which has a large extra burst of phosphate release (Gilbert et al., 1995; Moyer et al., 1998).

The rate of dissociation of the MtMC1 complex

The MtMC1 complex was dissociated by ATP and ADP at higher ionic strength (100 mM NaCl) or lower protein concentration. The rate of dissociation was measured by the decrease in 90° light scattering. A typical signal is plotted in Fig. 5 *a* (2.5 μM tubulin, 5 μM MC1 heads, 0.5 mM ATP, concentrations after mixing). The particular curve has a small deviation from a single exponential term, although some traces give a satisfactory fit to a single exponential. This small slow process with rate constant less than 1 s^{-1}

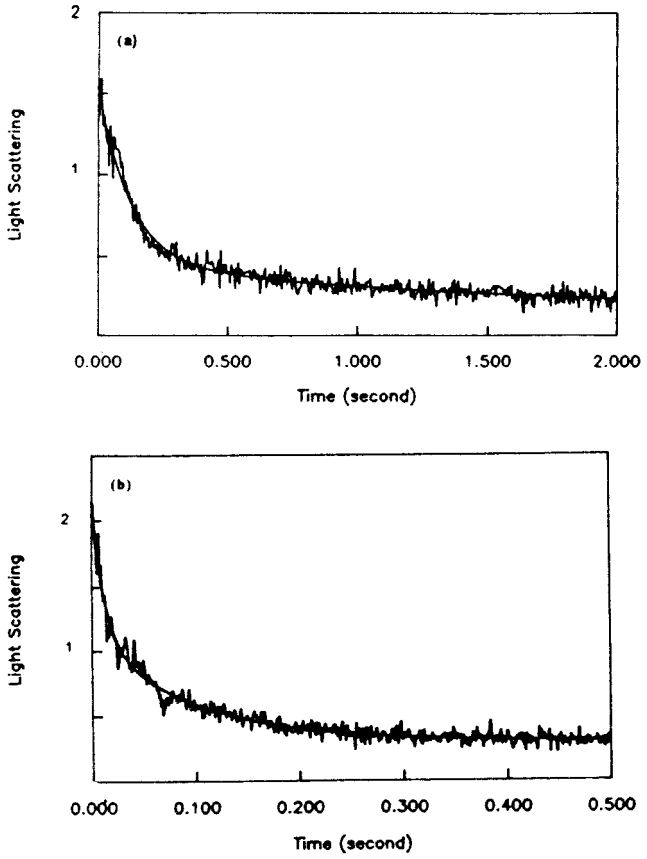

FIGURE 5 (*a*) Dissociation of the MtMC1 complex by ATP. MtMC1 complex, 5 μM MC1, 2.5 μM Mt, was reacted with 500 μM ATP. The jagged curve is the 90° light scattering signal at 295 nm and the smooth curve is the best fit to two exponential terms with rate constants of 8.7 s^{-1} and 0.73 s^{-1}. (*b*) Dissociation of MtMC1 complex by ADP. Protein concentrations are the same as in (*a*). MtMC1 was reacted with 500 μM ADP. The smooth curve is the best fit to two exponential terms with rate constants of 81 and 7.1 s^{-1}. Conditions: standard buffer, 100 mM NaCl, 21°C. MtMC1 was pretreated with apyrase to remove bound nucleotide. Light scattering is plotted on an arbitrary scale; the decrease in scattering intensity is 14% for the reaction with ATP and 17% for reaction with ADP

may arise from baseline drift. The rate constant of dissociation was 9 $\pm$ 1 $s^{-1.}$ The rate constant was independent of ATP concentration for concentrations greater than 0.1 mM.

These measurements were made with MC1 heads in excess of microtubule sites. The occupancy of the microtubule was approximately one head per tubulin dimer based on the sedimentation assay. The fractional change in light scattering, $-\Delta V/V_{\text{initial}}$, was typically 0.15. After correction for scattering from the buffer, the fractional change is at least 0.3. If light scattering is roughly proportional to mass per unit length a decrease of 0.45 is expected. Therefore, the signal amplitude is the range expected for the dissociation of the MtMC1 complex.

The rate of dissociation was essentially the same at an occupancy of 0.5 heads per dimer, although the signal amplitude was reduced by 40%. In 50 mM NaCl, the rate of dissociation was 12 s^{-1}, but the amplitude was reduced further because the complex was not completely dissociated. This increase in the observed rate is consistent with a contribution from the rate of reassociation.

In these experiments the MtMC1 complex was treated with apyrase to remove bound ADP. Omission of the apyrase treatment reduced the amplitude of the light scattering signal, but it was still fitted by a single exponential term with rate constant of 11 $\pm$ 1 s^{-1}.

The rate constant of dissociation of the MtMC1 complex by ATP is essentially the same as for the MtNcd monomer complex, within experimental error (Pechatnikova and Taylor, 1997). The MtMC1 complex that was not treated with apyrase has at least one ADP bound per dimer, as described in the next section. The results are consistent with MC1 being bound to the microtubule by only one head; consequently, the rate of dissociation does not depend on whether the second head is occupied by ADP.

The dissociation by ADP of an MtMC1 complex with one MC1 head per tubulin dimer, gave a biphasic signal (Fig. 5 *b*). The larger rate constant of 90 $\pm$ 15 s^{-1} contributed 60% to 70% of the signal. The slower process with rate constant of 8 $\pm$ 3 s^{-1} is in the same range as the rate constant for dissociation by ATP. The larger rate process was also observed at one-half occupancy of microtubule sites; therefore, the large value is not attributed to repulsive interaction between dimers. The significance of the biphasic signal is not clear. It is unlikely that the larger rate process measures some change in orientation of the two heads of the dimer, because the change in light scattering should be determined mainly by the mass per unit length. A larger rate of dissociation by ADP versus ATP was also observed for a microtubule–kinesin monomer complex (Ma and Taylor, 1997a). We cannot rule out a change in microtubule aggregation as a source of the fast process until dissociation can be measured by another technique such as fluorescence energy transfer, which is under investigation. ADP appears to dissociate the MtMC1 complex at least as fast as ATP and probably much faster.

The ADP dissociation step

It has been shown for monomeric Ncd and for the MC5 dimer (Lockhart et al., 1995) that the rate constant of mant ADP release from the microtubule complex is slightly larger than the steady-state rate. The apparent rate constant of mant ADP dissociation was measured by mixing MC1·mant ADP with microtubules in the absence of ATP or in the presence of ATP to block mant ADP rebinding. The decrease in fluorescence is shown in Fig. 6 at a microtubule concentration of 10 μM. In the absence of ATP, the amplitude of the decrease in fluorescence was only about 30% as large as in the presence of ATP. However the apparent rate of the process appears to be larger because the fit to one exponential term gave a rate constant of 4 s^{-1} in the absence of ATP and 0.7 s^{-1} in the presence of ATP. In Fig. 6, relative fluorescence is plotted on an arbitrary scale that is proportional to photomultiplier output voltage. The fractional change in fluorescence in the presence of ATP,

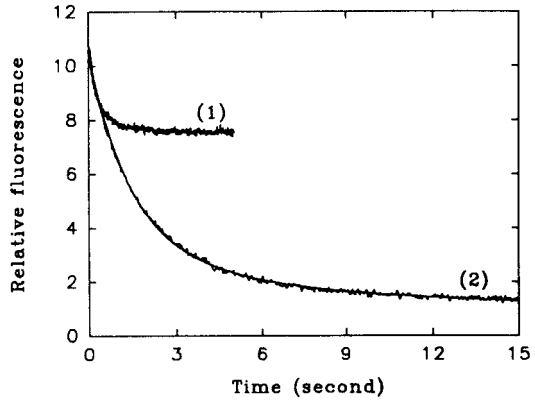

FIGURE 6 Dissociation of mant ADP from MC1 by binding to microtubules. The MC1·mant ADP complex at a concentration of 4 μM was reacted with 10 μM microtubules (final concentrations) in the absence or presence of ATP. Curve 1, microtubules alone; Curve 2, microtubules plus 1 mM ATP. Approximately 30% of the mant ADP was released in the absence of ATP. The rate constant is 4 s^{-1} in the absence of ATP compared to 0.7 s^{-1} in the presence of ATP, based on fitting to one exponential term. Conditions; standard buffer, 50 mM NaCl, 22°C.

$-\Delta V/V_{initial}$, is 0.35. The expected value for complete dissociation of mant ADP is 0.38 for a fluorescence enhancement ratio of 1.6; consequently, the signal measures the release of mant ADP from both heads of the dimer.

The fluorescence transient for the reaction of MC1·mant ADP with microtubules in the absence of ATP was fitted by one exponential term plus a linear term, which contributed less than 15% of the signal amplitude. The rate of the linear phase was essentially independent of microtubule concentration, and this signal probably is the result of photobleaching because there was a slow loss of intensity over the same time range when MC1·mant ADP was mixed with buffer. The apparent rate constant is plotted in Fig. 7. The value increased with microtubule concentration with an initial slope $k^a = 0.5\ \mu M^{-1}\ s^{-1}$ and reached a maximum value of at least 9 s^{-1}. The smooth curve in Fig. 7 is the fit to a hyperbola, which gives a rate constant of 12 s^{-1}.

The fluorescence signal for the reaction of MC1·mant ADP with microtubules plus ATP could only be fitted approximately by one exponential plus a linear term. The maximum rate constant was only 1.4 s^{-1} and the dependence on concentration gave a $k^a < 0.1\ \mu M^{-1}\ s^{-1}$. These values are not consistent with the results obtained in the absence of ATP. The large rate of dissociation of the first molecule of mant ADP should be the same whether or not ATP is present.

The signal-to-noise ratio of the fluorescence signal is high, which justifies fitting the data to two exponential terms plus a linear term. The contribution of the linear term was at most 10% of the total signal, and the rate did not depend on microtubule concentration. An example of the fit of the fluorescence transient by two exponential terms is shown in Fig. 8 for a microtubule concentration of 60 μM. The two apparent rate constants are plotted versus microtubule concentration in Fig. 7. The values obtained at the

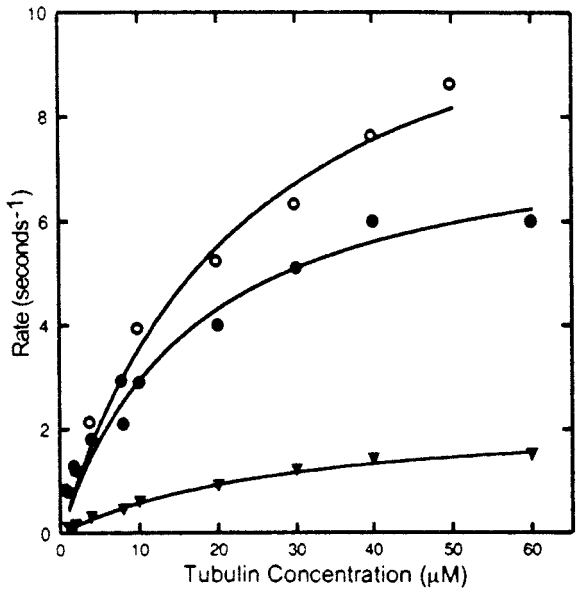

FIGURE 7 Dependence of the rate of dissociation of mant ADP on microtubule concentration. The fluorescence transient, in the absence of ATP (○) was fitted to one exponential plus a linear term that is attributed to photobleaching. In the presence of 500 μM MgATP, the transient was fitted to two exponential terms (●, ▼) plus a linear term. The process with the larger rate constant contributed 25% of the signal amplitude at 2 μM microtubule site concentration and 35% at 60 μM. Conditions as in Fig. 6, except that the MC1·mant ADP concentration ranged from 1 μM for the lowest microtubule concentration to 2.5 μM at higher microtubule concentrations. The smooth curves are hyperbolas fitted to the data by a nonlinear least squares program (sigma plot).

highest microtubule concentrations are 6 s^{-1} for the larger rate constant and 1.5 s^{-1} for the smaller. The larger rate process contributed 25% of the signal amplitude at the lowest microtubule concentration, which increased to 35% at the highest concentration. The fit of the data to a hyper-

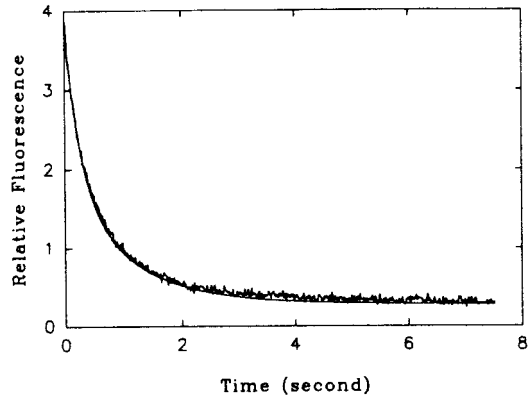

FIGURE 8 Rate of Dissociation of mant ADP by microtubules in the presence of ATP. The MC1·mant ADP complex was mixed with microtubules plus ATP. The fit of the fluorescence decrease to two exponential terms is illustrated by the smooth curve. The rate constants are 6 and 1.4 s^{-1}. An additional linear decrease equal to 10% of the total change in fluorescence is caused by photobleaching. Conditions; standard buffer, 50 mM NaCl, 2.5 μM MC1·mant ADP, 60 μM microtubules, 500 μM MgATP.

bola gives rate constants of 8 s^{-1} and 2.3 s^{-1} for the two processes. However the kinetic scheme discussed in the Conclusions section need not yield a hyperbolic dependence on microtubule concentration, and the processes are compared in terms of the observed values.

It is evident that the larger rate constant agrees with the rate constant obtained in the absence of ATP, at least over the range from low-to-moderate microtubule concentrations. The maximum rate of mant ADP dissociation in the absence of ATP is significantly higher than the larger rate process in the presence of ATP. However, the observed rate constant in the absence of ATP includes a contribution from the rate of rebinding of mant ADP because the process does not go to completion. Also, the fit to two exponentials plus a linear term involves six parameters, and the values of the rate constants are affected by the choice of this function to represent the data. It is concluded that the two measurements of the rate constant of dissociation of the first mant ADP are in reasonable agreement.

The behavior of MtMC1 is similar to conventional kinesin (Hackney, 1994; Ma and Taylor, 1997b). The dimer binds to the microtubule by one head, and mant ADP dissociates from the attached head. The second head cannot interact with the microtuble, and the binding of ATP to the first head is required to release mant ADP from the second head. Therefore, the dissociation of the two molecules of mant ADP is a sequential process.

Although the results are similar to dimeric kinesin, there are significant differences in the kinetic behavior. In the kinesin case, the rate of dissociation of mant ADP from the MtK·mant ADP complex by the binding of ATP to the other head is an order of magnitude larger than the rate of dissociation of kinesin from the microtubule. Therefore, a direct interaction between the heads is necessary to explain the results (Ma and Taylor, 1997b). In the MtMC1 case, the observed rate of dissociation of the second mant ADP is much smaller than the rate of dissociation of the MC1 from the microtubule by ATP. Therefore, the dissociation of mant ADP from the second head could proceed by an indirect pathway. After release of the first mant ADP, the MtMC1·mant ADP complex is dissociated by ATP into Mt plus MC1·mant ADP·ATP. This complex can rebind to the microtubule by the mant ADP-containing head, followed by the dissociation of the mant ADP. Further experiments were carried out to distinguish between the direct and indirect pathways.

The pathway of dissociation of the second mant ADP

The critical difference between the direct and indirect pathways is that the latter requires the dissociation and rebinding of MC1·mant ADP to accelerate the rate of release of mant ADP. First, it is necessary to determine the rate of the spontaneous dissociation of mant ADP from the detached head in the absence of ATP. When MC1·mant ADP is mixed with microtubules, less than half of the mant ADP is released. This result suggests that a fraction of the mant ADP is still bound to the attached head, in addition to the mant ADP that is strongly bound to the detached head. To distinguish between the two complexes, we compared the rates of dissociation of mant ADP from the MtMC1· mant ADP complex by ATP versus apyrase. Measurements were made in a fluorimeter because the rate of dissociation of mant ADP from the detached head is too small to measure in a stop-flow apparatus.

The addition of 5 μM microtubules to 1 μM MC1· mant ADP dimer reduced the fluorescence by 25 to 30% compared to the total change observed in the presence of excess ATP (Fig. 9). The final fluorescence level compared to the fluorescence of 1 μM mant ADP showed that, initially, 0.8 M mant ADP were bound per MC1 site. The number is not corrected for impurities, inactive MC1, or incomplete exchange of mant ADP for ADP. Essentially, the MC1 dimer bound 2 M mant ADP. Therefore, binding of the MC1·mant ADP complex to the microtubule released 0.5 to 0.6 M mant ADP per mole of dimer. Addition of 20 units per mL of apyrase to the complex released an additional 0.4 to 0.5 M mant ADP per dimer by a fast process that was not tracked by the fluorimeter, while the remainder of the mant ADP dissociated at a rate of 0.003 s^{-1}. The value ranged from 0.003 to 0.005 s^{-1} in several experiments. Therefore, one mant ADP is bound very tightly to the MtMC1 dimer (dissociation constant of 10^{-8} M calculated from the rate constants of mant ADP binding and dissociation).

The rate of the fast process obtained by the addition of apyrase to an MtMC1·mant ADP complex was also mea-

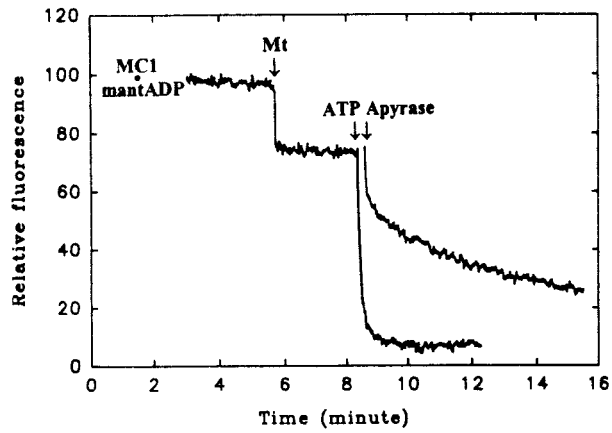

FIGURE 9 Comparison of the rates of dissociation from the two classes of mant ADP binding sites. 1 μM MC1·mant ADP was mixed with 5 μM microtubules (final concentrations) and then with 1 mM ATP or 10 units per mL apyrase. Because of the long time interval, measurements were made by hand mixing using an MPF-44A fluorimeter. The addition of microtubules released 25 to 30% of the mant ADP. All of the remaining mant ADP was released by ATP by a fast process. In a second experiment, apyrase was added instead of ATP. The trace starts at the same level but it was displaced along the time axis to separate it from the ATP trace. Apyrase released the remainder of the weakly bound mant ADP by a fast process. The second mole of mant ADP dissociated at a rate of 0.003 s^{-1} from the strongly bound site. Conditions; standard buffer, 50 mM NaCl, 22°C. Fluorescence is plotted on an arbitrary scale; the total change in fluorescence corresponds to a 40% decrease relative to the value at zero time.

sured in the stop-flow apparatus. A rate constant of 2 s^{-1} was obtained by mixing MtMC1·mant ADP with apyrase at a concentration of 10 units/mL and a rate constant of 5 s^{-1} at 20 units/mL, which indicates that the fast step is at least 5 s^{-1}. The same experiment done with ATP gave a rate constant of 5 to 10 s^{-1} for the fast phase. The remainder of the mant ADP was released at a rate of 0.5 s^{-1}. Therefore, the fast process shown in Fig. 9 for the addition of apyrase is the spontaneous dissociation of the remainder of the mant ADP bound to the attached head.

The behavior of MtNcd monomer was compared with that of the MtMC1 dimer. At an Ncd monomer·mant ADP concentration of 4 μM, 75% of the mant ADP was released by mixing with 10 μM microtubules. The remainder of the mant ADP was dissociated by either ATP or apyrase at a rate of 1.5 to 2 s^{-1}(data not shown).Therefore part of the mant ADP bound to MtMC1 and all of the mant ADP that remained bound to the MtNcd monomer is in equilibrium with free mant ADP with a dissociation constant in the μM range. The slow mant ADP dissociation step obtained with the MC1 dimer, but not with the monomer, corresponds to release of mant ADP from the second head, which is probably detached because the rate constant of mant ADP dissociation is only three or four times larger than for free MC1.

The direct mechanism for mant ADP release from the second head by the binding of ATP predicts that the rate of dissociation of the mant ADP is independent of microtubule concentration. An MtMC1·mant ADP complex, formed from 2 μM MC1·mant ADP and 2 μM microtubules, was mixed 1:1 with 1 mM ATP plus increasing concentrations of microtubules. The fluorescence signal was fitted by two exponential terms. The smaller rate constant, which corresponds to the release of the second mant ADP, increased with microtubule concentration essentially as shown in Fig. 7. An objection to the design of the experiment is that, in forming the complex of MC1·mant ADP with microtubules, some MC1·mant ADP remains dissociated from microtubules in the presence of a low concentration of free mant ADP. The rebinding of this dissociated MC1·mant ADP could partly account for the dependence of the rate constant on microtubule concentration.

A better test of the reaction pathway was made by determining the effects of AMPPNP and ADP on the release of the second mant ADP using the experimental protocol described in Fig. 9. The addition of 5 μM microtubules to 2 μM MC1·mant ADP released approximately 30% of the bound mant ADP. The addition of 1 mM AMPPNP gave the same result as the reaction with apyrase shown in Fig. 9. After a relatively fast release of some mant ADP, which is weakly bound, the second mant ADP dissociated very slowly with a rate constant of 0.004 s^{-1}. AMPPNP does not dissociate the protein complex, and it appears to act simply as a competitor to block mant ADP rebinding. The results suggest that dissociation of the MC1·mant ADP complex from the microtubule is a necessary step for the release of the mant ADP. In the kinesin case, AMPPNP released the second mant ADP by the direct pathway at a rate of 30 s^{-1} (Ma and Taylor, 1997b).

The experiment was repeated with ADP, and all of the mant ADP was released by a relatively fast process whose rate was too large to measure in the fluorimeter. Stop-flow measurements of the reaction of MC1·mant ADP with microtubules plus 1 mM ADP gave results that were the same as for ATP. The fluorescence signal fitted two exponential terms with maximum values of 10 and 1 s^{-1}.

In the kinesin case, the rate of dissociation of the second mant ADP by ADP was only 2 to 3 s^{-1} compared to more than 100 s^{-1} by ATP. Because ADP rapidly dissociates the MtMC1 complex, the results are consistent with the indirect pathway. The slow release of mant ADP by ADP in the kinesin case can also be explained by the indirect pathway.

CONCLUSIONS

The objective of this study is to determine the steps in the microtubule-MC1 ATPase mechanism and to compare the scheme with that of a monomeric Ncd motor domain. Measurements were made at high microtubule concentrations compared to the K_M for microtubule activation or to the K_d in the presence of ATP. Although a small fractional dissociation cannot be prevented, the rate constants refer to the associated MtMC1 complex. The structural evidence, as well as the kinetic evidence presented here, indicates that MC1 is bound to the microtubule by only one head. A kinetic scheme is proposed for the attached head, which is consistent with most of the evidence. We then consider how the scheme is to be modified to take account of the detached head.

$$\mathrm{MtN} + \mathrm{T} \underset{k_{-1}}{\overset{k_1=110\mathrm{s}^{-1}}{\rightleftharpoons}} \mathrm{MtN{\cdot}T} \overset{k_2=20\mathrm{s}^{-1}}{\rightleftharpoons} \mathrm{MtN{\cdot}D{\cdot}P}$$

$$\overset{k_3=10\mathrm{s}^{-1}(-\mathrm{P})}{\rightleftharpoons} \mathrm{MtN{\cdot}D} \underset{k_{-4}=200\mathrm{s}^{-1}}{\overset{k_4=6\mathrm{s}^{-1}}{\rightleftharpoons}} \mathrm{MtN} + \mathrm{D}$$

Scheme 1

where T, D, and P refer to nucleoside triphosphate, nucleoside diphosphate, and inorganic phosphate, respectively. MtN refers to the complex of one head of the MC1 dimer with a microtubule binding site. ATP and ADP bind to the complex with an apparent second-order rate constant of 2 μM^{-1} s^{-1}, which is typical of nucleotide binding reactions. A weakly bound collision complex is formed in the reaction, but this step is omitted for simplicity; k_1 and k_{-4} refer to the maximum rate of the isomerization step induced by binding of the nucleotide.

Values assigned to k_2, k_3, and k_4 are based on measurements of the phosphate burst, phosphate dissociation, and mant ADP dissociation steps, but the values are partly dependent on a model. The rate of the phosphate burst is 23 s^{-1}. This rate is equal to k_2 plus the effective rate of product release ($k_3k_4/(k_3 + k_4)$). Because the effective rate is 2 to 3

s^{-1}, the value of k_2 is slightly larger than 20 s^{-1}. This value agrees with that for monomeric Ncd and therefore refers to the attached head.

The rate constant of phosphate dissociation (k_3) is affected by partial dissociation of the protein complex, which occurs at a rate of 10 s^{-1}. The measured rate of 9 s^{-1} may slightly underestimate k_3, and a value of 10 s^{-1} is assigned to this step.

The rate of dissociation of mant ADP (k_4) was obtained from the reaction of MC1·mant ADP with microtubules in the absence of ATP, and also from fitting the transient in the presence of ATP to two exponential terms. Values for different preparations were in the range of 8 to 10 s^{-1} and 6 to 7 s^{-1} for the two methods. It is concluded that the rate constant of mant ADP dissociation is at least 6 s^{-1}.

The rate constants k_1 and k_{-4} for the isomerization induced by binding of mant ATP and mant ADP respectively were obtained using nucleotide-free Ncd. In the case of mant ADP, the Ncd monomer and the MC1 dimer gave the same values for k_{-4} and the apparent second-order rate constant k^a; consequently, these rate constants must be similar for the attached and detached heads of the dimer. The difference is in the rate of mant ADP dissociation, which is 6 s^{-1} for the attached head and 0.004 ± 0.001 s^{-1} for the detached head.

The monomer and dimer showed different kinetic behavior for the binding of mant ATP, which requires an explanation in terms of the two heads. The increase in fluorescence fitted two exponential terms at low substrate concentrations (Fig. 2 *b*), but the amplitude of the term with the smaller rate constant decreased with substrate concentration. The detached head is expected to have a higher affinity for mant ATP than the attached head; consequently it will dominate the fluorescence signal at very low substrate concentrations. However the value of k^a is very similar for monomer and dimer. Therefore, the binding step is similar for attached and detached heads of the dimer and the difference is in a larger value of k_{-1}.

A lower affinity for mant ATP of the attached head is indicated by the value of K_M(ATP) of 25 μM and a value of V_M/K_M(ATP) of approximately 0.1 μM^{-1} s^{-1}. Scheme 1 for the attached head predicts two exponential terms for the fluorescence transient at low substrate concentrations. If the concentration of substrate is similar to the dissociation constant for the first step, k_{-1}/k^a, the binding site is not saturated in the first step, and the transition from MtN·T to MtN·D·P will yield a further increase in fluorescence. This qualitative explanation is supported by simulation of the mechanism. The rate equations can also be solved by making the approximation $k_e = k_3k_4/(k_3 + k_4)$ where k_e is the effective rate constant of product release (Ma and Taylor, 1995). The rate constants assigned to Scheme 1 and the values of k_{-1} in the range 30 to 50 s^{-1} account for the dependence of the smaller rate constant on concentration of substrate and also for the decrease in amplitude of the signal at higher substrate concentrations.

Other lines of evidence are consistent with binding of the dimer to the microtubule by a single head. The dissociation constants of the MtMC1 complex in the presence of ATP, ADP, and other nucleotides are reduced by approximately a factor of two compared to monomeric Ncd. A factor of at least two is expected for a dimer that can bind by either head; consequently, the second head is contributing little or nothing to the binding affinity. Also, the rate of dissociation of the MtMC1 complex by ATP or ADP has no lag phase, and it is essentially the same as the rate for the monomer.

MC1 exhibits the same property as kinesin in that only one ADP is released on binding to the microtubule, whereas the second ADP is dissociated by the addition of ATP. However the kinetic behavior is significantly different. The rate constant for the dissociation of the second mant ADP is only 1.5 s^{-1} compared to at least 6 s^{-1} for the rate of dissociation of the first mant ADP. The evidence suggests that the main pathway for the dissociation of the second mant ADP involves dissociation and rebinding of the MC1·mant ADP complex to the microtubule. It is proposed that the pathway is

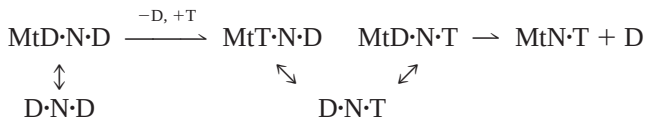

Scheme 2

The symbols MtT·N·D and MtD·N·T indicate that the dimer is bound through the T- or D-containing head, respectively. The scheme requires that the rate constant of ADP dissociation is the same for the release of the first and second molecules of ADP. The mechanism was simulated for a range of rate constants using KINSIM (dissociation of ADP, 8 s^{-1}: dissociation of T·N·D bound by T-head, 5 to 10 s^{-1}, equilibrium dissociation constant, 5 μM; dissociation of D·N·T or D·N·D bound by D-head, 20 to 50 s^{-1}, equilibrium dissociation constant, 10 μM). The simulated curves fitted two exponential terms, and the rate constants increased with microtubule concentration to maximum values of 8 s^{-1} and 1 to 2 s^{-1}. The term with the larger rate constant contributed 30 to 40% of the signal over the range of microtubule concentrations in agreement with the experimental results. Intuitively, D·N·T could rebind by either head, but only the MtD·N·T complex releases ADP and the observed rate constant must be less than half the actual rate constant. If a direct pathway is included, that is MtT·N·D ⟷ MtN·T + D, the rate constant of this step must be less than 1 to 2 s^{-1}. Otherwise the scheme will not explain the amplitude of the term with the smaller rate constant.

The results are consistent with an alternating head mechanism. The maximum ATPase rate per head was less than 2 s^{-1} per MC1 site, which is approximately half as large as the rate for the Ncd monomer. The rate constants assigned to Scheme 1 give a maximum steady-state rate of 3 to 4 s^{-1} per head. Because only one head of the dimer cycles at a

time, the observed rate is 1.5 to 2 s^{-1} for an alternating head mechanism.

The reaction pathway and processivity

Motility measurements have not demonstrated processive motion for dimeric Ncd. It is less than the lower limit of five steps, detectable by the single molecule assay (Case et al., 1997). Three tests have been used for kinetic processivity.

The apparent second-order rate constant obtained from the ratio of k_{cat}/K_M(Mt) is larger than 10^8 M^{-1} s^{-1} for processive kinesin, which indicates many ATPase cycles per encounter (Hackney, 1995).The value for MC1 is less than 10^6 M^{-1} s^{-1} in the present work. A larger value was obtained by Crevel et al. (1997) at a lower ionic strength, but the authors also concluded that the motor has low processivity.

A second measure of processivity is the ATPase turnover rate divided by the rate of dissociation of the microtubule-motor complex by ATP. The ratio is less than one in 50 mM salt, which indicates low processivity.

A third measure is the size of the phosphate burst under conditions such that the microtubule–motor complex is largely dissociated when the steady state is reached (Gilbert et al., 1995; Ma and Taylor, 1997a; Jiang and Hackney, 1997; Moyer et al., 1998)). Based on the intercept of the steady-state rate plot at zero time, a burst of at most 1.5 phosphate per site was obtained.

In addition, models of processive motion require the binding of ATP to the attached head to release ADP from the second head without dissociation of the dimer from the microtubule (Ma and Taylor, 1997b). The results on MC1 showed that dissociation of the dimer by ATP or ADP followed by rebinding to the microtubule was the main pathway for release of mant ADP from the detached head.

The various lines of kinetic evidence show that MC1 has little or no processivity.

The kinetic pathway and the direction of motion

The differences in relative values of the rate constants for Ncd and kinesin raise the possibility that the reaction pathway is different for the two motors. Are these differences in rate constants important in determining the direction of motion, or do they reflect some other property that distinguishes between these two motors? Motion is generated by a change in structure in a transition between two attached states that must be reversed at some other step to complete the ATPase cycle. The reversal is expected to occur between detached states to obtain efficient coupling of the hydrolysis cycle to motion. Reversal of direction could be obtained kinetically if one motor followed the pathway shown by the dashed arrows and the other followed the pathway shown by the solid arrows

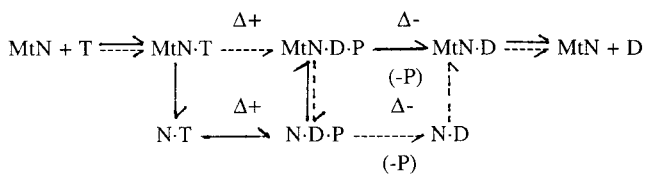

A positive structural change Δ+, is defined as a transition that can be coupled to a step in the positive direction along the microtubule. The kinetic mechanism requires ADP release to take place in an attached state, which is followed by ATP binding to the attached state. Because these steps are common to both pathways, the structural changes can only be assigned to the hydrolysis and phosphate release steps in a model that seeks to give a kinetic-pathway explanation of the direction of motion.

Kinesin could follow the pathway indicated by the dashed arrows; ATP binding to MtK, hydrolysis (a positive change), dissociation of the K·D·P state, phosphate release (a negative change), and binding of K·ADP to the microtubule. This pathway corresponds to one of the pathways proposed by Gilbert et al. (1995). A reasonable criterion for the choice of a particular path is a ratio of ten for the rate constants at a branch point. The rate constant of the hydrolysis step of kinesin is at least ten times larger than the rate constant of dissociation of kinesin from the microtubule by ATP.

The only remaining choice to obtain kinetic-reversal of direction for Ncd is the pathway shown by the solid arrows. The rate of dissociation of MtMC1 by ATP is 10 s^{-1}, whereas the rate constant of the hydrolysis step is only 20 s^{-1}. In part, MtMC1 could follow the pathway of dissociation by ATP followed by hydrolysis. A burst of phosphate release was obtained for MtN·D·P, but the rate of dissociation of phosphate from N·D·P is not an order of magnitude smaller than from MtN·D·P. Also, the N·D·P state is probably weakly bound to microtubules and it's rate of dissociation from the microtubule is comparable to the rate of phosphate dissociation from MtN·D·P. The ratios of rate constants at the branch points are too small to support the proposal that the main pathway for Ncd is that shown by the solid arrows. It is concluded that the direction of motion is not determined by differences in the reaction pathways of Ncd and kinesin.

The direction of motion appears to be related to differences in structure of the neck region and its interaction with the catalytic core that positions the free head to the positive (kinesin) or negative (Ncd) side of the bound head relative to the polarity of the microtubule (Hirose et al., 1996; Sosa et al., 1997; Hoeniger et al., 1998). However the evidence is not conclusive in the case of kinesin.

It is still necessary to explain how this asymmetry is used. Monomeric kinesin moves with low efficiency in the positive direction (Berliner et al., 1995; Young et al., 1998), which implies that there are intrinsic structural changes in the cycle. A small structural change of the monomer, to-

gether with the asymmetry of the dimer, probably biases attachment of the second head to give an 8-nm step.

The direction of motion, in this view, is determined by an opposite change in structure for the same step in the kinetic scheme or by the structural change occurring at a different step in the cycle. The differences in the kinetic behavior still suggest a difference in the mechanisms of Ncd and kinesin. A useful parameter for characterizing motor mechanisms is the ratio of the mechanical velocity (U) to the maximum ATPase turnover rate (V_M) per head, $U/V_M = D$, where D has the dimensions of distance traveled per ATP hydrolyzed per head. The value of D for myosin is 300 to 400 nm based on measurements using myofibrils (Ma and Taylor, 1994). A large value of D is characteristic of a nonprocessive motor that spends a small fraction of its cycle time in a force-generating state. This fraction is termed the duty-cycle ratio R. We define R as, $R = d/D$ where d is the step size for unloaded motion. This definition is equivalent to that of Uyeda et al. (1990). The relationship of R to the actomyosin kinetic scheme has been treated in Ma and Taylor (1994).

Kinesin has a D value of approximately 15 nm (Romberg et al., 1998). The step size is 8 nm for the movement of the center of mass, but possibly 16 nm for the step size per head (Hua et al., 1997; Schnitzer and Block, 1997), which means the duty-cycle ratio is close to one. A value near unity is expected of a highly processive motor that spends most of the cycle time exerting a force (Howard, 1997; see also Young et al., 1998).

Ncd has a velocity of 100 to 200 nm s^{-1} (Chandra et al., 1993; Schimizu et al., 1995a) and an ATPase of 1.5 s^{-1}. D is approximately 100 nm and R is 0.08 to 0.16, depending on whether Ncd takes an 8- or 16-nm step per head. Therefore, Ncd appears to behave like a nonprocessive motor with a relatively low duty-cycle ratio.

The kinetic scheme is capable of explaining the velocity of Ncd. The step in the cycle that is coupled to force or motion is unknown. We assume it is ADP dissociation or the fast transition that is induced by ATP binding. Because the N·ADP state dissociates rapidly from the microtubule, the MtN·ADP complex would exert only a small drag. The steps are: binding of N·D by a single head, ADP release and ATP binding that generates the force or movement, and hydrolysis, which is followed by rapid dissociation to terminate the force.

$$\mathrm{MtN{\cdot}D} \underset{-\mathrm{D},\,+\mathrm{T}}{\overset{6\mathrm{s}^{-1}}{\longrightarrow}} \mathrm{MtN{\cdot}T} \overset{20\mathrm{s}^{-1}}{\longrightarrow} \mathrm{MtN{\cdot}D{\cdot}P} \overset{\mathrm{fast}}{\longrightarrow} \mathrm{Mt} + \mathrm{N{\cdot}D\ (P)}$$

Multiple nonprocessive motors generate a maximum velocity $U = k_f d$, where k_f is the rate constant of the force-terminating step (Ma and Taylor, 1994). k_f is 20 s^{-1}, and d is assumed to be 8 nm because the system takes only one step. These values give $U = 160$ nm s^{-1}. The single head has a turnover rate of 3 s^{-1}, therefore $R = 0.15$, which agrees with the experimental results.

We wish to thank Aldona Rukuiza for expert technical assistance. We also thank T. Shimizu for helpful discussion of the relation of the velocity of motion to the ATPase activity of Ncd.

This work was funded by a grant from the National Institutes of Health (GM-51858 to EWT)

REFERENCES

Berliner, E., C. Young, K. Anderson, H. Matani, and J. Gelles. 1995. Failure of a single-headed kinesin to track parallel to microtubule protofilaments. *Nature.* 373:718–721.

Brune, M., J. L. Hunter, J. E. Corrie, and M. R. Webb. 1994. Direct real time measurement of rapid inorganic phosphate release using a novel fluorescent probe. *Biochemistry.* 33:8262–8271.

Case, R. B., D. W. Pierce, N. Hom-Booher, C. L. Hart, and R. D. Vale. 1997. The directional preference of kinesin motors is specified by an element outside the motor catalytic domain. *Cell.* 90:959–966.

Chandra, R., E. D. Salmon, H. P. Erickson, A. Lockhart, and S. A. Endow. 1993. Structural and functional domains of the *Drosophila* Ncd microtubule motor protein. *J. Biol. Chem.* 268:9005–9013.

Crevel, I. M., A. Lockhart, and R. A. Cross. 1996. Weak and strong states of kinesin and Ncd. *J. Mol. Biol.* 257:66–76.

Crevel, I. M., A. Lockhart, and R. A. Cross. 1997. Kinetic evidence for low chemical processivity in Ncd and eg5. *J. Mol. Biol.* 273:160–170.

Foster, K. A., J. J. Correia, and S. P. Gilbert. 1998. Equilibrium binding studies of non-claret disjunction protein (Ncd) reveal cooperative interactions between motor domains. *J. Biol. Chem.* 273:35307–35318.

Gilbert, S. P., M. R. Webb, M. Brune, and K. A. Johnson. 1995. Pathway of processive ATP hydrolysis by kinesin. *Nature.* 373:671–676.

Gilbert, S. P., M. L. Moyer, and K. A. Johnson. 1998. Alternating site mechanism of the kinesin ATPase. *Biochemistry*. 37:792–799.

Endow, S. A., and K. W. Waligora. 1998. Determinants of kinesin motor polarity. *Science*. 281:1200–1202.

Hackney, D. D. 1994. Evidence for alternating head catalysis by kinesin during microtubule stimulated ATP hydrolysis. *Proc. Nat. Acad. Sci. USA.* 91:6865–6869.

Hackney, D. D. 1995. Highly processive microtubule-stimulated ATP hydrolysis by dimeric kinesin head domains. *Nature.* 377:448–450.

Henningsen, U., and M. Schliva. 1997. Reversal in the direction of movement of a molecular motor. *Nature.* 389:93–95.

Hirose, K., A Lockhart, R. A. Cross, and L. A. Amos. 1996. Three dimensional cryoelectron microscopy of dimeric kinesin and Ncd motor domains on microtulules. *Proc. Nat. Acad. Sci. USA.* 93:9539–9544.

Hoenger, A., S. Sack, M. Thormahlen, A. Marx, J. Muller, H. Gross, and E. Mandelkow. 1998. Image reconstructions of microtubules decorated with monomeric and dimeric kinesins: comparison with x-ray structure and implications for motility. *J. Cell Biol.* 141:419–430.

Hua, W., E. C. Young, M. L. Flemming, and J. Gelles. 1997. Coupling of kinesin steps to ATP hydrolysis. *Nature.* 388:390–393.

Howard, J. 1997. Molecular motors: structural adaptation to cellular function. *Nature.* 389:154–158.

Jiang, W., and D. D. Hackney. 1997. Monomeric kinesin head domains hydrolyze multiple ATP molecules before release from a microtubule. *J. Biol. Chem.* 272:5616–5621.

Kozielski, F., S. Sack, A. Marx, M. Thormahlen, E. Schonbrunn, V. Biou, A. Thompson, E. M. Mandelkow, and E. Mandelkow. 1997. The crystal structure of dimeric kinesin and implications for microtubule-dependent motility. *Cell*. 91:985–994.

Kull, F. J., E. P. Sablin, R. Lau, R. J. Fletterick, and R. D. Vale. 1996. Crystal structure of the kinesin motor domain reveals a structure similar to myosin. *Nature.* 380:550–555.

Lockhart, A., R. A. Cross, and D. F. McKillop. 1995. ADP release is the rate limiting step of the MT activated ATPase of non-claret disjunctional and kinesin. *FEBS Lett.* 368:531–535.

Lockhart, A., and R. A. Cross. 1996. Kinetics and motility of the eg5 microtubule motor. *Biochemistry.* 35:2365–2373.

Ma, Y. Z., and E. W. Taylor. 1994. Kinetic mechanism of myofibril ATPase. *Biophys. J.* 66:1542–1553.

Ma, Y. Z., and E. W. Taylor. 1995. Mechanism of microtubule kinesin ATPase. *Biochemistry.* 34:13242–13251.

Ma, Y. Z., and E. W. Taylor. 1997a. Kinetic mechanism of a monomeric kinesin construct. *J. Biol. Chem.* 272:717–723.

Ma, Y. Z., and E. W. Taylor. 1997b. Interacting head mechanism of microtubule-kinesin ATPase. *J. Biol. Chem.* 272:724–730.

Moyer, M. L., S. P. Gilbert, and K. A. Johnson. 1998. Pathway of ATP hydrolysis by monomeric and dimeric kinesin. *Biochemistry.* 37: 800–813.

Pechatnikova, E., and E. W. Taylor. 1997. Kinetic mechanism of monomeric non-claret disjunctional protein. *J. Biol. Chem.* 272:30735–30740.

Romberg, L., D. W. Pierce, and R. D. Vale. 1998. Role of kinesin neck region in processive microtubule based motility. *J. Cell Biol.* 140: 1407–1416.

Sablin, E. P., F. J. Kull, R. Cooke, R. D. Vale, and R. J. Fletterick. 1996. Crystal structure of the motor domain of Ncd. *Nature.* 380:555–559.

Sablin, E. P., R. B. Case, S. C. Dai, C. L. Hart, A. Ruby, R. D. Vale, and R. J. Fletterick. 1998. Direction determination in the minus-end-directed kinesin motor Ncd. *Nature.* 395:813–816.

Schnitzer, M. J., and S. M. Block. 1997. Kinesin hydrolyses one ATP per 8 nm step. *Nature.* 388:386–390.

Shimizu, T., Y. Y. Toyoshima, M. Edamatsu, and R. D. Vale. 1995a. Comparison of the motile and enzymatic properties of two microtubule minus-end-directed motors, Ncd and cytoplasmic dynein. *Biochemistry.* 34:1575–1582.

Shimizu, T., E Sablin, R. D. Vale, R. Fletterick, E. Pechatnikova, and E. W. Taylor. 1995b. Expression, purification, ATPase properties and microtubule binding properties of the Ncd motor domain. *Biochemistry.* 34: 13259–13266.

Sosa, H., D. P. Dias, A. Hoenger, M. Whittaker, E. Wilson-Kubalek, E. Sablin, R. J. Fletterick, R. D. Vale, and R. A. Milligan. 1997. A model of the microtubule-Ncd motor protein complex. *Cell.* 90:217–224.

Uyeda, T. Q. P., S. J. Kron, and J. A. Spudich. 1990. Myosin step size. *J. Mol. Biol.* 214:699–710.

Vale, R. D., T. Funatsu, D. W. Pierce, L. Romberg, Y. Harada, and T. Yanagida. 1996. Direct observation of single kinesin molecules moving along microtubules. *Nature.* 380:451–453.

Young, E. C., H. K. Mahtani, and J. Gelles. 1998. One head kinesin derivatives move by a nonprocessive, low duty ratio mechanism. *Biochemistry.* 37:3467–3479.